IEICE Proceeding Series

A Numerical Study on Electroporation by Amplitude-Modulated Electric Field

Yoshihiko Susuki

Vol. 2 pp. 479-482
Publication Date: 2014/03/18
Online ISSN: 2188-5079

2013 International Symposium on Nonlinear Theory and its Applications
NOLTA2013, Santa Fe, USA, September 8-11, 2013

A Numerical Study on Electroporation by Amplitude-Modulated Electric Field

Yoshihiko Susuki

Department of Electrical Engineering, Kyoto University
Katsura, Kyoto 615–8510 Japan
susuki.yoshihiko.5c@kyoto-u.ac.jp

Abstract—We study dynamics of electroporation in a single spherical cell exposed to Amplitude-Modulated (AM) electric fields. This study is based on the mathematical model of electroporation developed in [Krassowska and Filev, Biophys. J., vol.92, pp.404–417, 2007]. Numerical simulations of the model suggest that an AM electric field induces the electroporation and a created pore substantially evolves under the AM field.

1. Introduction

Electroporation is a multiscale phenomenon of biological cell membrane in which its electrical permeability changes due to creation of transient pores by electric pulses [1, 2]. This phenomenon is widely used in medicine and biotechnology, because it enables the delivery of biologically active molecules, which are normally impermeable through ion channels, into cells. Recent advance of microfludics enables the development of single cell electroporation devices [3].

The purpose of this paper is to investigate the use of alternating electric fields to induce the electroporation. Normal electroporation is induced with an electric field with constant amplitude. It is recognized in [3] that a strong electric field induces the *irreversible* electroporation, that is, damages a cell. In contrast to this, our approach presented in this paper is based on *alternating* electric fields. The use of alternating electric fields has a potential of decreasing the damage of cells and of inducing the fluid movement in a micro-scale channel (see e.g, [4, 5]), which enables the development of novel microfludic electroporation devices in which electroporation, separation, and detection processes of cells are integrated. Several groups of researchers have studied on electroporation by alternating electric fields: see e.g. [6, 7, 8]. In [9] the authors develop a nonlinear dynamical system model for electroporation of a single spherical cell exposed to electric fields. In this paper, based on the developed nonlinear model, we numerically study multiscale phenomena in the dynamics of electroporation induced by an Amplitude-Modulated (AM) electric field.

2. Dynamical Model

We briefly introduce the dynamical model of electroporation of a single spherical cell exposed to electric fields, which is developed in [9]. Fig. 1 shows the schematic diagram of electroporation of a single cell. For deriving the model, we make the following assumptions: (i) system is under electro-quasistatic state; (ii) parameters of the cell membrane are constant; and (iii) changes of cell area, volume, and shape are negligible. No space for explaining all parameters of the model is available in this paper: see [9] in details. According to the spatial symmetry posed in the problem, the dynamical model here is derived for a two-dimensional object. However, in order to compute the number of pores around the cell, we will consider the three-dimensional cell surface.

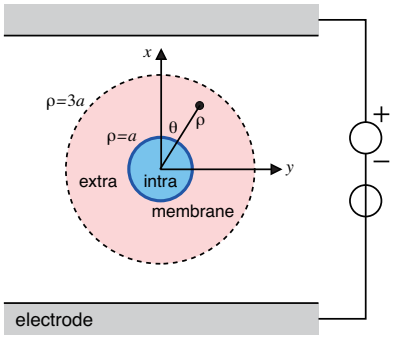

Figure 1: Schematic diagram of electroporation of a single spherical cell suspended in conductive fluid. The polar coordinate (ρ, θ) is used for mathematical modeling. The intercell region Ω_{i} is given as $\{(\rho,\theta); 0 \le \rho < a\}$ and the outercell region Ω_{e} fulfilled by conductive fluid as $\{(\rho,\theta); a < \rho < 3a\}$. The cell membrane $\partial\Omega_{\mathrm{m}}$ corresponds to $\{(\rho,\theta); \rho = a\}$ and the outer boundary $\partial\Omega$ to $\{(\rho,\theta); \rho = 3a\}$.

The electrostatic potentials $\phi_{\mathrm{i}}(t,\rho,\theta)$ and $\phi_{\mathrm{e}}(t,\rho,\theta)$ inside and outside the cell, denoted by Ω_{i} and Ω_{e}, are represented by the following Laplace's equations:

$$\epsilon_{\mathrm{i}}\nabla^2\phi_{\mathrm{i}} = 0 \ \text{ in } \ \Omega_{\mathrm{i}}, \ \ \epsilon_{\mathrm{e}}\nabla^2\phi_{\mathrm{e}} = 0 \ \text{ in } \ \Omega_{\mathrm{e}}, \tag{1}$$

with the boundary conditions as

$$\begin{aligned} s_{\mathrm{i}}(-\nabla\phi_{\mathrm{i}})\cdot\boldsymbol{e}_\rho &= s_{\mathrm{e}}(-\nabla\phi_{\mathrm{e}})\cdot\boldsymbol{e}_\rho \ \text{ on } \ \partial\Omega_{\mathrm{m}}, \\ &= C_{\mathrm{m}}\partial_t v_{\mathrm{m}} + g_1(v_{\mathrm{m}} - V_{\mathrm{rest}}) + j_{\mathrm{ep}}, \quad (2) \\ \phi_{\mathrm{e}} &= -3ae(t)\cos\theta \ \text{ on } \ \partial\Omega, \quad (3) \end{aligned}$$

where $\nabla^2 = \partial_{\rho\rho} + \partial_\rho/\rho + \partial_{\theta\theta}/\rho^2$, $\nabla = \boldsymbol{e}_\rho\partial_\rho + \boldsymbol{e}_\theta\partial_\theta/\rho$, and $\partial\Omega_{\mathrm{m}}$ denotes the cell membrane and $\partial\Omega$ the outer Dirichlet boudary (see Fig. 1). The function $v_{\mathrm{m}}(t,\theta)$ is the transmembrane potential defined as $\phi_{\mathrm{i}}(t,a,\theta) - \phi_{\mathrm{e}}(t,a,\theta)$, and $j_{\mathrm{ep}}(t,\theta)$ the current density through pores at time t and angle θ. The control variable $e(t)$ stands for the input electric field and V_{rest} for the rest potential. The constant s_{i} (or s_{e}) denotes

the conductivity of medium inside (or outside) the cell. The boundary condition on the cell membrane $\partial\Omega_{\rm m}$ is based on the equation of current continuity along ρ-axis.

The dynamics of number density of pores on the cell membrane, denoted by $n_{\rm ep}(t,\theta)$, are represented by the following differential equation:

$$\partial_t n_{\rm ep} = \alpha {\rm e}^{(v_{\rm m}/V_{\rm ep})^2}\left\{1-(n_{\rm ep}/N_0){\rm e}^{-q(v_{\rm m}/V_{\rm ep})^2}\right\}. \quad (4)$$

The current through one pore with radius r at time t and angle θ, denoted by $i_{\rm ep}(t,\theta;r)$, is represented by

$$i_{\rm ep}(t,\theta;r) = v_{\rm m}(t,\theta)/\{R_{\rm ep}(r)+2R_{\rm in}(r)\}, \quad (5)$$

where we introduce the two resistances $R_{\rm ep}(r) := h/(\pi s r^2)$ and $R_{\rm in}(r) := 1/(4sr)$. In actual simulations, the surface of cell is discretized in θ from 0 to π with length $\Delta\theta$. Let us denote by A_i a potion of the cell area for each discrete angle θ_i. The total current through pores inside a small portion A_i at time t, denoted as $j_{\rm ep}(t,\theta_i)A_i$, is approximately represented by

$$j_{\rm ep}(t,\theta_i)A_i \approx \sum_{j=1}^{N_i(t)} i_{\rm ep}(v_{\rm m}(t,\theta_i);r_j), \quad (6)$$

where we write $i_{\rm ep}$ as a function of the transmembrane potential $v_{\rm m}$, because it is uniquely determined by $v_{\rm m}$ and r. Here the number $N_i(t)$ of pores in A_i is defined as $[\int_{A_i} n_{\rm ep}{\rm d}A]$, where $[\bullet]$ denotes the floor function over $\mathbb{R}$. Then, we have the current density $j_{\rm ep}(t,\theta_i)$ at time t and discrete angle θ_i as follows:

$$j_{\rm ep}(t,\theta_i) = \sum_{j=1}^{N_i(t)} \frac{i_{\rm ep}(v_{\rm m}(t,\theta_i);r_j)}{A_i}. \quad (7)$$

It is here supposed that each pore is initially created with radius r^* and changes its size to minimize the energy of the entire membrane. For a cell with pores of the total number $N(t) = [\int_A n_{\rm ep}{\rm d}A]$ at time t (where A denotes the cell surface with area $4\pi a^2$), the time evolution of j-th pore with radius r_j at angle θ is represented by

$$\dot{r}_j = -\frac{D}{k_{\rm B}T}\frac{\partial}{\partial r_j}W(\boldsymbol{r}, v_{\rm m}(t,\theta), \sigma_{\rm eff}(\boldsymbol{r})), \quad (8)$$

where $j = 1,2,\ldots,N(t)$, $\dot{r}_j := {\rm d}r_j/{\rm d}t$, $r_j \geq r^*$, and $\boldsymbol{r} := [r_1, r_2, \ldots, r_{N(t)}]^\top$ (where $\top$ denotes the transpose operation of vectors). The function W stands for the total energy of cell membrane, given as

$$\begin{aligned} W(\boldsymbol{r}, v_{\rm m}(t,\theta), \sigma_{\rm eff}) &= \sum_{j=1}^{N(t)}\left\{-\int_0^{r_j} F(r_j, v_{\rm m}(t,\theta_j)){\rm d}r \right. \\ &\left. +\beta(r^*/r_j)^4 + 2\pi\gamma r_j - \pi\sigma_{\rm eff}r_j^2\right\}. \end{aligned} \quad (9)$$

The first term on the right-hand side denotes the contribution of transmembrane potential $v_{\rm m}$ to energy. The function F is the electric force acting on a discrete pore with toroidal geometry, given as

$$F(r, v_{\rm m}) = \frac{F_{\rm max}}{1+r_{\rm h}/(r+r_{\rm t})}v_{\rm m}^2. \quad (10)$$

The second term accounts for the Steric repulsion of lipid heads in the membrane, the third term for the edge energy of pore perimeter, and the fourth term for the effect of membrane tension to energy. The quantity $\sigma_{\rm eff}$ is the effective tension of the membrane, given as

$$\sigma_{\rm eff}(\boldsymbol{r}) = 2\sigma' - \frac{2\sigma'-\sigma_0}{(1-A_{\rm ep}/A)^2}, \quad A_{\rm ep} = \sum_{j=1}^{N(t)}\pi r_j^2. \quad (11)$$

The dynamical system described by (1), (4), and (8) is infinite-dimensional, nonlinear, and hybrid, because it contains a quantized operation. The dimension of the part of phase space spanned by pore radii $\boldsymbol{r}$ changes as time increases. In this paper, we perform numerical simulations of the system by applying an appropriate discretization technique in space and time to it.

3. Numerical Simulations

We perform numerical simulations of the model in order to investigate the use of AM electric field to induce the electroporation. The protocol of input electric field $e(t)$ is firstly introduced in Sec. 3.1. Results on numerical simulations of the model are described in Secs. 3.2 and 3.3.

3.1. Protocol of Input Electric Field

In this study, determining the protocol of input electric field $e(t)$ is crucial. In the transitional electroporation process, the following electric field with constant amplitude E is used:

$$e(t) = E. \quad (12)$$

Here we consider the following protocol of input electric field:

$$e(t) = E\left\{1+\epsilon\sin\left(\frac{2\pi}{T}t+\varphi\right)\right\}, \quad (13)$$

where ϵ denotes the modulation factor, T the modulation period, and φ its initial phase. The protocol in the case of $\epsilon = 0$ corresponds to the transitional one with constant amplitude.

The period T of the AM electric field is determined as follows. Under a constant electric field E, the transmembrane potential $v_{\rm m}(t,\theta)$ for the first passive charging process without electroplated pore is represented in [9] by

$$v_{\rm m}(t,a,\theta) = \frac{3}{2}aE(1-{\rm e}^{-t/\tau})\cos\theta + V_{\rm rest}, \quad (14)$$

where τ denotes the time constant given by

$$\tau = aC_{\rm m}\left(\frac{1}{s_{\rm i}}+\frac{1}{2s_{\rm e}}\right). \quad (15)$$

The existence of τ possibly affects the electroporation exposed to alternating electric fields. In the parameter setting of [9], the value of τ is 1.45 μs. According to the critical value τ, we choose T and use the parameters of input electric field summarized in Tab. 1. Here we choose the maximum value of AM electric field in comparison with the case of constant electric field: see Fig. 2A. The other parameters in the model are fixed at the same values as in [9].

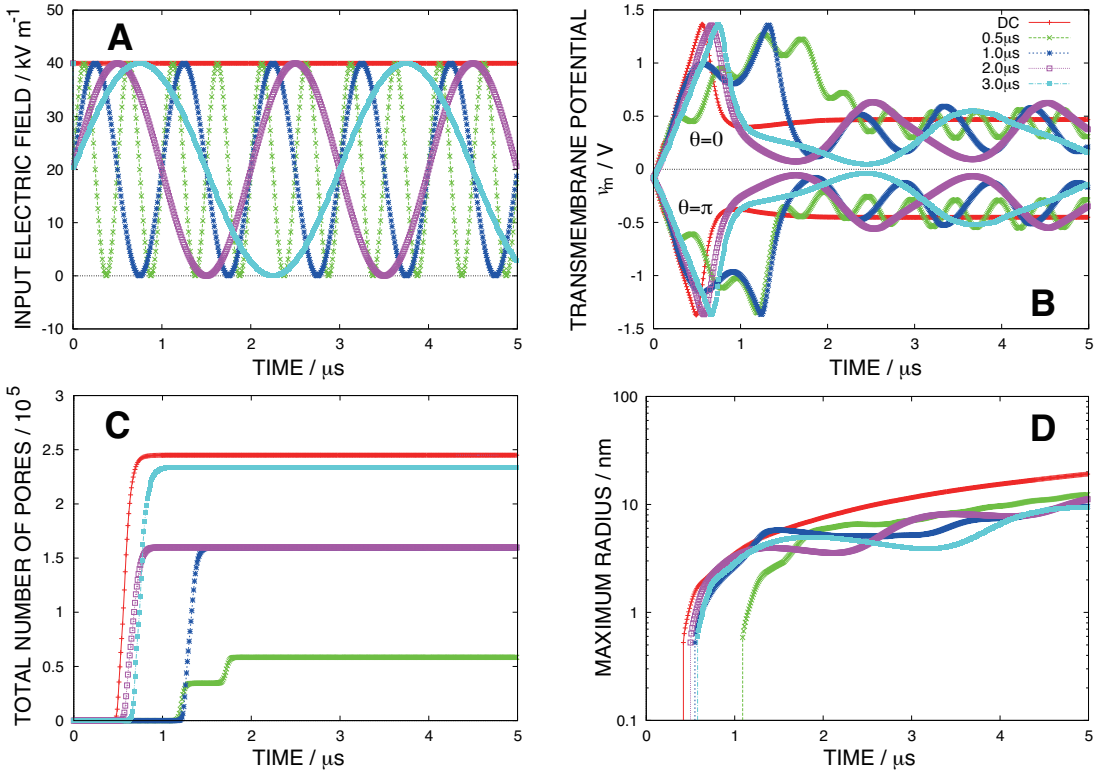

Figure 2: Numerical simulations of short-term dynamics in electroporation of a single spherical cell exposed to electric fields: (A) input electric fields; (B) transmembrane potentials at $\theta = 0$ and π; (C) total number of pores; and (D) maximal radius of pore.

Table 1: Parameters of input electric field

parameter	value	
E	40 kV/m	(constant case)
	20 kV/m	(AM case)
ϵ	1	
T	0.5 μs, 1 μs, 2 μs, 3 μs	
φ	0 rad	

3.2. Short-term Dynamics

First, we investigate short-term dynamics of the electroporation process up to a few micro seconds, in which the cell membrane is passively charged and multiple pores are created. Fig. 2 presents numerical results on the short-term dynamics from 0 s to 5 μs. The input electric fields $e(t)$ are shown in Fig. 2A. The time changes of transmembrane potentials $v_{\mathrm{m}}(t, \theta)$ at $\theta = 0$ (depolarized pole in the case of constant field) and π (hyper polarized pole), total number of pores, and maximum radius are also shown in Figs. 2B, C, and D. The results in the case of constant field, denoted by a *red* line, are reported in Fig. 2 of [9]. Note that the results are slightly different because of the choice of cell portion A_i and the difference of numerical methods. Due to the alternating nature of $e(t)$, the transmembrane potentials in Fig. 2B behave in an oscillatory manner. In Fig. 2C, the total number of pores change in a different manner among the four cases, and the number of pores in the case of $T = 3\,\mu$m becomes close to that in the case of constant field. Also, in Fig. 2D, the maximum radii grow in both cases of constant and modulated fields. These results imply that an AM electric field induces the electroporation.

3.3. Mid-term Dynamics

Next, we investigate mid-term dynamics of the electroporation from a few micro seconds to a mili second, in which the created pores evolve. Fig.3 shows the time evolution of pore distributions that is sampled at 30 μs, 100 μs, and 1 ms. The three cases are shown in (A) constant field, (B) AM field at $T = 1\,\mu$s, and (C) at $T = 3\,\mu$s. Here we do not plot the number of pores with radii of less than 2 ns, which form a dominant group in pore distributions. The results in the case of constant field, denoted by A, are reported in Fig. 4 of [9]. The distributions evolve with time in both the cases of constant and modulated fields. The peak of distributions around radius $r = 20$ ns appears for both the cases. These suggest that a created pore evolves under an AM electric field.

4. Concluding Remarks

In this paper, we have investigated the multiscale phenomenon of electroporation in a single spherical cell exposed to AM electric fields. Numerical simulations of the model suggest that an AM electric field induces the electroporation and a created pore substantially evolves under the AM electric field.

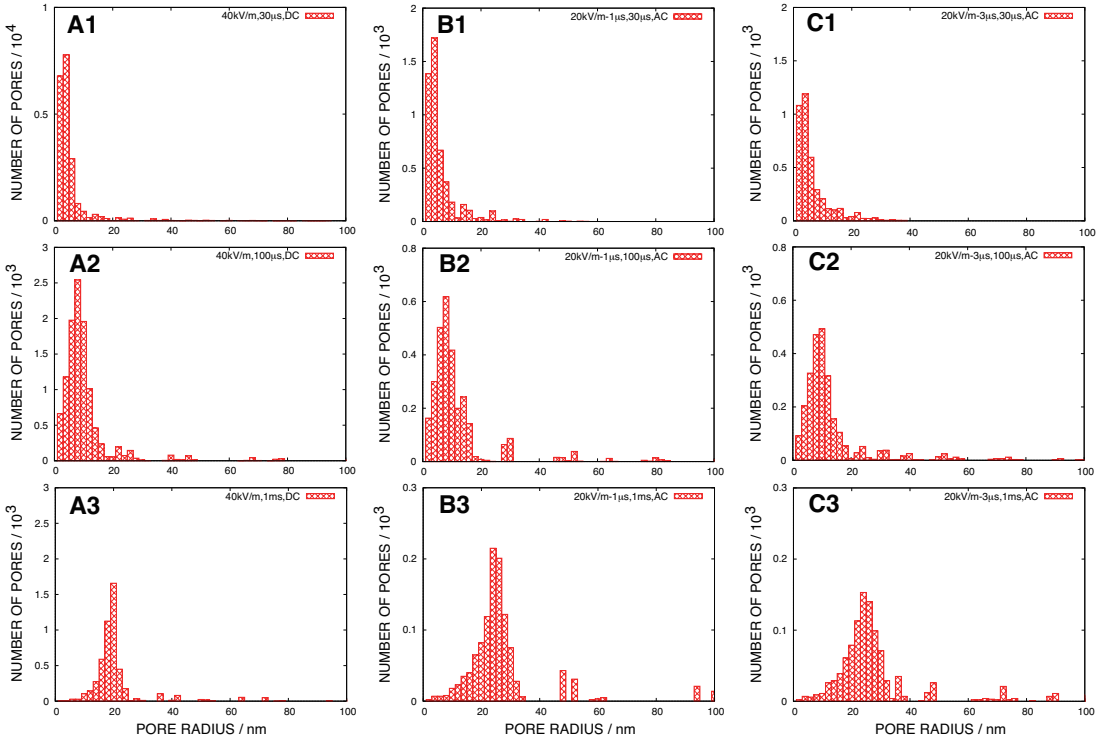

Figure 3: Numerical simulations of mid-term dynamics in electroporation of a single spherical cell exposed to electric fields. Time evolution of pore distributions is traced in the cases of (A) constant field, (B) AM field at $T = 1\,\mu$s, and (C) at $T = 3\,\mu$s.

Many follow-up studies of this work exist: (i) simulations of long-term dynamics on the resealing of pores and (ii) multiphysics simulations of the phenomenon by considering the change of cell shape and the movement of conductive fluid. The former topic in (ii) is related to electrohydrodynamics of a giant vesicle [10, 11], which is a candidate material of experimental valuation of the current work.

Acknowledgements

I would like to appreciate Professor Igor Mezić (UC Santa Barbara) for introducing me to research on electroporation with references [2, 9]. I am also grateful to Mr. Jun Nishimura (Kyoto University) for his assistance of numerical simulations and to reviewers for their valuable comments of the manuscript. The work was supported in part by MEXT KAKENHI Grant Number 23760390 and Itoh Chubei Foundation.

References

[1] E. Neumann, A. E. Sowers, and C. A. Jordan, editors. *Electoporation and electrofusion in cell biology*. Plenum Press, New York, 1989.

[2] J. C. Weaver and Y. A. Chizmadzhev. *Bioelectrochemistry and Bioenergetics*, 41:135–160, 1996.

[3] M. B. Fox, D. C. Esveld, A. Valero, R. Luttge, H. C. Mastwijk, P. V. Bartels, A. van den Berg, and R. M. Boom. *Analytical and Bioanalytical Chemistry*, 385:474–485, 2006.

[4] A. Ramos, M. Morgan, N. G. Green, and A. Castellanos. *Journal of Physics D: Applied Physics*, 31:2338–2353, 1998.

[5] A. González, A. Ramos, N. G. Green, A. Castellanos, and M. Morgan. *Physical Review E*, 61(4):4019–4028, April 2000.

[6] S. Movahed and D. Li. *Microfluid Nanofluid*, 10:703–734, 2011.

[7] S. Talele, P. Gaynor, J. van Ekeran, and M. J. Cree. In Magued Iskander, Vikram Kapila, and Mohammad A. Karim, editors, *Technological Developments in Education and Automation*, pages 355–359. Springer, 2010.

[8] S. Talele, P. Gaynor, M. J. Cree, and J. van Ekeran. *J. Electrostatics*, 10:261–274, 2010.

[9] W. Krassowska and P. D. Filev. *Biophysical Journal*, 92:404–417, January 2007.

[10] R. Dimova, K. A. Riske, S. Aranda, N. Bezlyepkina, R. L. Knorr, and R. Lipowsky. *Soft Matter*, 3:817–827, 2007.

[11] P. M. Vlahovska, R. S. Graciá, S. Aranda-Espinoza, and R. Dimova. *Biophysical Journal*, 96:4789–4803, June 2009.